VIP Fluorescent Probes Very Important Paper

How to cite: *Angew. Chem. Int. Ed.* **2021**, *60*, 16900–16905
International Edition: doi.org/10.1002/anie.202104100
German Edition: doi.org/10.1002/ange.202104100

Cyanine-Dyad Molecular Probe for the Simultaneous Profiling of the Evolution of Multiple Radical Species During Bacterial Infections

*Zhimin Wang[+], Thang Do Cong[+], Wenbin Zhong, Jun Wei Lau, Germain Kwek, Mary B. Chan-Park, and Bengang Xing**

Abstract: *Real-time monitoring of the evolution of bacterial infection-associated multiple radical species is critical to accurately profile the pathogenesis and host-defense mechanisms. Here, we present a unique dual wavelength near-infrared (NIR) cyanine-dyad molecular probe (HCy5-Cy7) for simultaneous monitoring of reactive oxygen and nitrogen species (RONS) variations both in vitro and in vivo. HCy5-Cy7 specifically turns on its fluorescence at 660 nm via superoxide or hydroxyl radical ($O_2^{\bullet-}$, $^{\bullet}OH$)-mediated oxidation of reduced HCy5 moiety to Cy5, while peroxynitrite or hypochlorous species ($ONOO^-$, ClO^-)-induced Cy7 structural degradation causes the emission turn-off at 800 nm. Such multispectral but reverse signal responses allow multiplex manifestation of in situ oxidative and nitrosative stress events during the pathogenic and defensive processes in both bacteria-infected macrophage cells and living mice. Most importantly, this study may also provide new perspectives for understanding the bacterial pathogenesis and advancing the precision medicine against infectious diseases.*

Bacterial infections remain the worldwide challenge in recent decades, mainly due to the evolving pathogenicity, emergence of foreign pathogens and spread of antibiotic resistance.[1] Comprehensive efforts have been devoted to identify the infections pathogenesis, host defense and antibacterial mechanisms, which comprise the dynamic inflammatory response, immune activation as well as lethal actions.[2] Among the various bioactive factors in reference to infectious diseases, phagocyte-derived free radical species are widely implicated to play essential roles in the regulation of bacteria-induced inflammatory cascade and triggering intrinsic bactericidal effects.[3] Furthermore, several investigations have also demonstrated the imperative contributions of multiple radical mediators including reactive oxygen and nitrogen species (RONS, for example, $O_2^{\bullet-}$, $^{\bullet}OH$, H_2O_2, NO, $ONOO^-$, ClO^- etc.) towards the infection pathological development.[3a,4] However, conventional studies primarily relying on end-point analysis (EPA) such as histology and biochemical assays could not real-time monitor the complex interplay between radical status and pathological evolution of infections. The accessibility of the traditional strategies has also been impeded due to the processes of invasiveness, time consumption and risk of complications.[5] Therefore, simple, safe and effective methods are highly desired that would provide novel perspectives on precise diagnosis and therapeutic interventions.

As compared to EPA analyses, optical imaging techniques demonstrate the advantages of highly sensitive, noninvasive and time/cost-effective capacities for broad biomedical detections from the cellular (or molecular) level up to whole-body sections in living animals.[6] Furthermore, the diverse fluorescence sensors are emerging as powerful tools to investigate contagious diseases through specific targeting or responses of infection-associated bio-indicators including toxins, enzymes, inflammatory cytokines and other factors.[7] Particularly, some radical species-activated small molecular probes towards $O_2^{\bullet-}$, $^{\bullet}OH$, $NO^{\bullet}$, ClO^-, $ONOO^-$ etc. have been developed and readily utilized in fluorescence imaging of bacterial infection with superior specificity.[8] In spite of the great success for understanding the substantive relevance between those radical species and infections, detailed mechanisms of multi-radical variations in bacterial pathogenesis and host defense have not yet been exploited, mainly due to lack of multi-responsive imaging platforms. Recent studies have attempted to directly measure infection-induced oxidative and nitrosative stress status through bio-engineered redox-sensitive GFPs or the combination of different fluorescent probes,[9] however, these approaches are still limited by the inadequate multiplexing capacity, tissue penetration and unified sensing outcomes for real-time and simultaneous recognition of RONS dynamics during the pathological infection progression in vivo.

Here, we report a unique dual wavelength near-infrared (NIR) cyanine-dyad fluorescent molecular probe (HCy5-Cy7) for simultaneously monitoring of multiple radical species variations in vitro and in living mice. As illustrated in Scheme 1, upon the bacterial stimulation, HCy5-Cy7 specifically turns on its fluorescence at 660 nm due to the local overproduction of inflammation-associated $O_2^{\bullet-}$ or $^{\bullet}OH$ that triggers the oxidation of reduced cyanine moiety (HCy5) to conjugated Cy5, while the burst of $ONOO^-$ or ClO^- specie

[*] Z. Wang,[+] T. D. Cong,[+] J. W. Lau, G. Kwek, Prof. B. Xing
Division of Chemistry and Biological Chemistry, School of Physical & Mathematical Sciences, Nanyang Technological University
21 Nanyang link, 637371 Singapore (Singapore)
E-mail: Bengang@ntu.edu.sg
Prof. B. Xing
School of Chemical and Biomedical Engineering, Nanyang Technological University
70 Nanyang Drive, 637459 Singapore (Singapore)
Dr. W. Zhong, Prof. M. B. Chan-Park
School of Chemical and Biomedical Engineering, Nanyang Technological University
62 Nanyang Drive, 637459 Singapore (Singapore)
[+] These authors contributed equally to this work.
Supporting information and the ORCID identification number(s) for the author(s) of this article can be found under: https://doi.org/10.1002/anie.202104100.

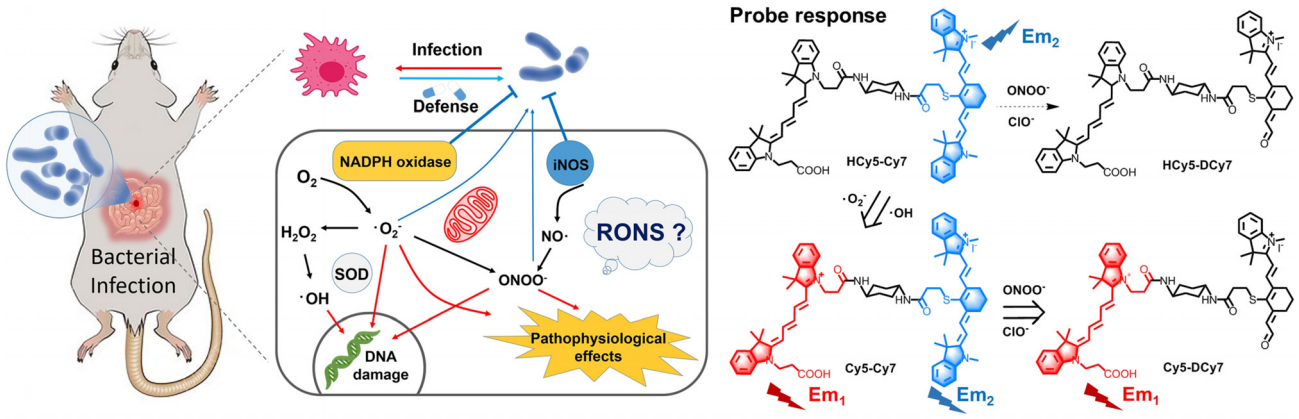

Scheme 1. Illustration of the pathogenesis and host defence of bacterial infections (left). Design and principle of HCy5-Cy7 for multiple radical species imaging (right): ROS oxidation of HCy5 to turn on the emission at 660 nm; RNS degradation of Cy7 to diminish the fluorescence at 800 nm. $\lambda_{Ex1/Em1} = 620/660$ nm, $\lambda_{Ex2/Em2} = 740/800$ nm.

induces Cy7 structural degradation, thereby leading to the emission depletion at 800 nm.[10] Such unique multispectral signal responses allow HCy5-Cy7 to investigate the dynamic oxidative/nitrosative stress and can thus correlate their evolutions with the pathogenic and defensive processes in bacterial infection both in vitro and in vivo.

We prepared the probe molecule HCy5-Cy7 by coupling hydroreductive Cy5 (e.g. HCy5) with Cy7 according to Scheme S1 (Supporting Information). Briefly, the dual carboxylic-substituted Cy5 was firstly synthesized, which was then reduced by $NaBH_4$ to obtain HCy5. In parallel, Cy7 fluorophore was modified with a cyclohexanediamine linker, thereby enabling its covalent link with the as-synthesized HCy5. The final molecule HCy5-Cy7 was purified with HPLC and characterized by NMR and mass spectroscopy (see the Supporting Information for details). Although cyanine dyes have been used for the sensitive detection of various biological radical species,[11] our rational design comes from the judicious integration of the $O_2^{\bullet-}$ and $^{\bullet}OH$ responsive HCy5 with $ONOO^-$-sensitive Cy7 that triggers the opposite fluorescence changes under two different spectral channels (e.g. at 660 nm and 800 nm), thus introducing the multiplexed recognitions of both ROS and RNS simultaneously. We envision that such a smart and multi-sensitive NIR fluorescent probe (HCy5-Cy7) could be particularly suitable for the arduous task of real-time multiple reactive species profiling, attribute to its synchronized biological distribution, metabolism as well as responsiveness.

Firstly, we tested the stability of HCy5-Cy7 in different environments such as PBS, PBS with 10% fetal bovine serum (FBS) or 10% human serum, and even cell culture DMEM (Dulbecco's Modified Eagle's-Medium) under dark or room light exposure. The measurements of absorption and fluorescence intensities at 660, 800 nm in Figure S1 proved that there is no obvious self-degradation of the Cy7 moiety or the auto-oxidation of the HCy5 part of our probe molecule. To validate the sensing ability of multiple radicals, the absorption and fluorescence spectra of HCy5-Cy7 were tested in PBS buffer with various radical species treatments. As shown in Figure 1a, the probe molecule only showed a major absorption peak at ≈780 nm attributing to the Cy7 chromophore. Upon $O_2^{\bullet-}$ reaction, a new peak was appeared at ≈640 nm, suggesting the structural conversion from HCy5-Cy7 to π-conjugation regenerated Cy5-Cy7 (Scheme 1). Differently, the addition of $ONOO^-$ led to a remarkable decrease of the absorption at ≈780 nm, which could be ascribed to the disruption of HCy5-Cy7 framework and the formation of truncated HCy5-DCy7. Furthermore, fluorescence responses of this probe with or without representative radical species

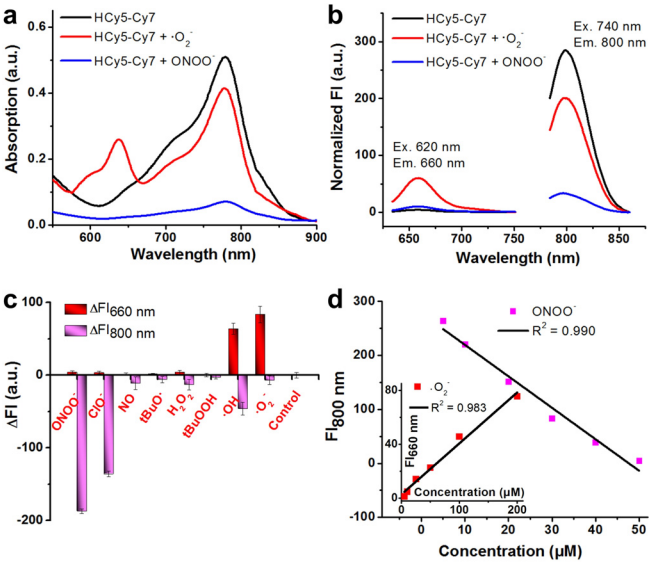

Figure 1. Multiple radical species detection via HCy5-Cy7. a) UV/Vis absorption and b) fluorescence spectra of HCy5-Cy7 (20 μM) in the absence or presence of $O_2^{\bullet-}$ (100 μM) or $ONOO^-$ (50 μM). c) The sensing specificity of HCy5-Cy7 towards different radical species (50 μM), including peroxynitrite ($ONOO^-$), hypochlorite (^-OCl), nitric oxide (NO), tert-butoxy radical ($^{\bullet}OtBu$), H_2O_2, *tert*-butyl hydroperoxide (TBHP), hydroxyl radical ($^{\bullet}OH$), and superoxide radical ($O_2^{\bullet-}$); $\Delta F = F_1 - F_0$, where F_1 indicates the fluorescence intensity of HCy5-Cy7 after RONS reaction, F_0 indicates the fluorescence intensity of HCy5-Cy7 alone. d) The fluorescence intensity fitting of HCy5-Cy7 as a function of $ONOO^-$ (or $O_2^{\bullet-}$, inset) concentration. $y = -5.83x + 278$ (blue); $y = 0.378x + 2.88$ (red).

(e.g. $O_2^{\bullet-}$ and $ONOO^-$) treatment were tested upon 620 and 740 nm excitations, respectively (Figure 1b). In comparison to HCy5-Cy7 alone, addition of $O_2^{\bullet-}$ induced the emission at ≈660 nm while $ONOO^-$ incubation significantly reduced the fluorescence signal at ≈800 nm, which were consistent with the absorption changes observed. In addition, the comparative studies of the photophysical properties between probe HCy5-Cy7 and the reference molecule Cy5-Cy7 further confirmed the specific probe structural conversion and related fluorescence responses (Figure S2). Although $O_2^{\bullet-}$ could cause a slight fluorescence decrease at 800 nm, the obvious dual- spectral responses were still able to identify ROS and RNS. As expected, HCy5-Cy7 demonstrated superb sensing specificity and multiplexed capability towards different radical species (Figure 1c). The fluorescence analysis exhibited opposite signal changes that HCy5-Cy7 treated with ROS (e.g. $O_2^{\bullet-}$ or $^{\bullet}OH$) resulted in a positive enhancement of the emission at 660 nm, whereas no obvious increase was observed upon the reaction with any other radical species. Meanwhile, fluorescence variations at 800 nm demonstrated a reverse trend after the reaction with RNS (e.g. $ONOO^-$ or ClO^-). In addition, both the fluorescence intensities at 660, 800 nm were linearly dependent with the concentrations of $O_2^{\bullet-}$ and $ONOO^-$ (Figure 1d), in which the limits of detection (LODs) were determined to be 0.34 and 0.082 μM, respectively. Such dual-channel and reversed fluorescent signal readout enabled HCy5-Cy7 as a multi-responsive reporter for simultaneous detection of multiple radical species in living system.

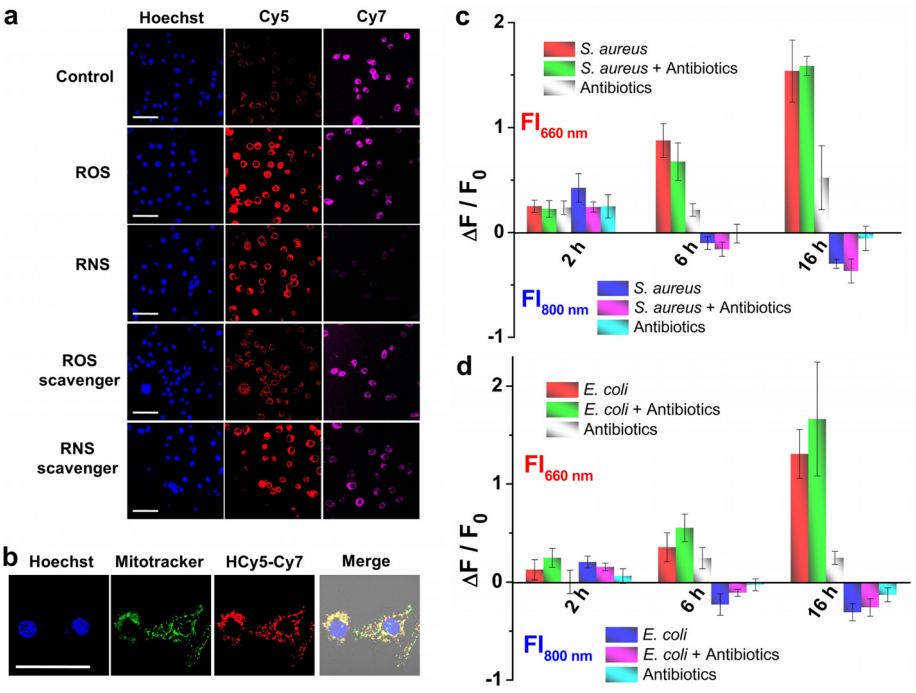

Figure 2. In vitro multiple radical species sensing. a) Fluorescence imaging of endogenous radical variations with HCy5-Cy7 (10 μM) in the RAW264.7 macrophage cells stimulated by PMA (0.2 μg mL^{-1}) or LPS/IFN-γ/PMA (2/0.05/0.01 μg mL^{-1}) accordingly. Blue = Hoechst 33342 (λ_{Ex} = 405 nm, λ_{Em} = 460/30 nm), Red = Cy5 channel (λ_{Ex} = 641 nm, λ_{Em} = 630/30 nm), violet = Cy7 channel (λ_{Ex} = 786 nm, λ_{Em} = 800/30 nm). Scale bars = 50 μm. b) Confocal analysis of HCy5-Cy7 cellular localization in PMA-stimulated RAW264.7 cells. Green = Mitochondria tracker (λ_{Ex} = 488 nm, λ_{Em} = 520/30 nm). Scale bar = 50 μm. c, d) The fluorescence intensity changes of HCy5-Cy7 (10 μM) incubated with RAW264.7 after gram-positive and gram-negative bacterial stimulations. $\Delta F = F_{bacteria} - F_{control}$, where $F_{bacteria}$ indicates the fluorescence intensity of HCy5-Cy7 incubated with RAW264.7 and bacterial cells, $F_{control}$ indicates the fluorescence intensity of HCy5-Cy7 incubated with RAW264.7 alone. F_0 indicates the fluorescence intensity of HCy5-Cy7 with RAW264.7/bacterial co-incubation at time t_0. Antibiotics: penicillin, 500 I.U. mL^{-1} and streptomycin, 500 μg mL^{-1}. The fluorescence intensities at 660 and 800 nm were measured with the excitation wavelength at 620 and 740 nm, respectively.

We then validated the feasibility of HCy5-Cy7 to monitor the endogenous multiple radical correlations in murine RAW264.7 macrophage cells. The specific cellular overproductions of $O_2^{\bullet-}$ and $ONOO^-$ were induced by chemical stimulations with phorbol 12-myristate 13-acetate (PMA) and lipopolysaccharide (LPS)/interferon-γ (IFN-γ)/PMA, respectively.[10a,11,12] Thereafter, the treated cells were incubated with the probe molecule for fluorescence confocal imaging analysis. As indicated in Figure 2a, the control cells treated with HCy5-Cy7 alone showed very weak fluorescence in the Cy5 channel (red) but strong fluorescence in the Cy7 channel (violet), clearly suggesting a low level RONS under normal conditions. However, a dramatic increase of red fluorescence can be observed in the PMA treated group and the violet fluorescence signal remained unchanged. These results demonstrated that HCy5-Cy7 could specifically detect cellular $O_2^{\bullet-}$ production, which was further confirmed by a negative control study with ROS scavenger pretreatment in the cells. Moreover, LPS/IFN-γ/PMA co-stimulated cells with HCy5-Cy7 addition exhibited a significant Cy5 fluorescence enhancement while the Cy7 fluorescence intensity was largely decreased with the signal close to the background, implying that both $O_2^{\bullet-}$ and $ONOO^-$ could be endogenously generated and detected in live cells. Although several studies proposed that LPS/IFN-γ/PMA stimulated macrophages could mostly induce $ONOO^-$ upregulation through the activation of NADPH oxidase and nitric oxide synthase (iNOS),[13] our cell stimulation studies together with the experiments treated with RNS scavenger clearly evidenced the coexistence and correlation of $O_2^{\bullet-}$ and $ONOO^-$ in the inflammatory process, which illustrated the importance of multi-responsive probes in the profiling of pathophysiology in complex and dynamic conditions. Besides, the HCy5-Cy7 probe molecule has also been proved to be able to target mitochondria and therefore enabled its possibility to precisely monitor in situ oxidation, nitrosation as well as subsequent cellular damages induced by

oxidative stress (Figure 2b). Moreover, in light with the negligible cytotoxicity of the probe (Figure S3), such unique multi-sensitive and compelling dual channel readout capabilities could also make HCy5-Cy7 more conducive to simultaneously manifest biological multi-radical variations in comparison with previously reported peroxynitrite- or superoxide-selective probes with their signal readout only under single spectral channel.[12,14]

Encouraged by the effective RONS imaging performance, HCy5-Cy7 was further applied to investigate the possibility of sensitive recognition multiple radical species evolutions in the host-defense process triggered by the invasion of bacterial pathogens. As proof of concept, we established the bacterial infection model through the typical stimulations of gram-positive (e.g. *S. aureus*) and gram-negative (e.g. *E. coli*) bacteria in the RAW264.7 macrophage cells.[9] Upon the incubation with bacteria, HCy5-Cy7 was applied to monitor the oxidative stress in macrophage cells. The dual wavelength fluorescence changes induced by bacteria infection at the different time duration in the comparison with control groups without bacteria were represented in Figure 2c and d. Generally, the fluorescence intensities at 660 nm in either *S. aureus* or *E. coli* incubated macrophages showed the similar time-dependent enhancement, demonstrating the obvious ROS production during the infection process. However, only slight fluorescence changes at 800 nm could be observed in both *S. aureus* and *E. coli* incubated cells, which suggested the possibility of the less RNS response along the bacteria contagion. To better understand whether the oxidative stress status was closely related to the interaction of bacteria with macrophage cells, we monitored the dynamic phagocytosis processes by using green fluorescent protein (GFP) labeled bacterial strains (Figure S4). To our surprise, the clear differences were observed that the phagocytosis of GFP/*S. aureus* was in a time-dependent manner, while GFP/*E. coli* showed less efficient uptake by RAW264.7 probably due to the distinct bacterial cell wall components. Such a phenomenon provided the evidence that the slight higher ROS enhancement in *S. aureus* infected microphages could be likely ascribed to the continuous stimulation of phagocytosis, yet *E. coli*-induced infection was more possibly due to endotoxin lipopolysaccharide (LPS)-mediated inflammatory stress.[15] Moreover, it should be noted that the antibiotics treatment of bacteria-infected macrophages slightly enhanced the ROS level in *E. coli* incubated cells, while antibiotics addition in *S. aureus* infected microphages cells triggered a small production of RNS radicals. These results implied that both ROS and RNS radical species played essential roles in the bacterial infection and antibiotics response,[9a] but the detailed biochemical mechanisms regarding the correlations of redox biology varying from bacterial strains, intracellular and intrabacterial redox-related signaling in infections still need to be further investigated.

Moreover, we further hypothesized that HCy5-Cy7 could also demonstrate a potential to study the multiplex redox biology of bacterial infection in living animals. Accordingly, the mice were intraperitoneally (*i.p.*) injected with living bacteria *E. coli* and *S. aureus*, respectively to induce the animal infections. After 2 h bacterial stimulation, the probe molecule was injected via tail vein (*i.v.*) and animal imaging was carried out over the time in an IVIS system (Figure 3 and Figure S5). As shown in Figure 3a and c, the fluorescence at 660 nm channel in the infected mice showed a significant enhancement as comparison with saline-treated controls, such ROS enhancement under this spectral window reached the maximum response upon 2 h post probe injection. At this

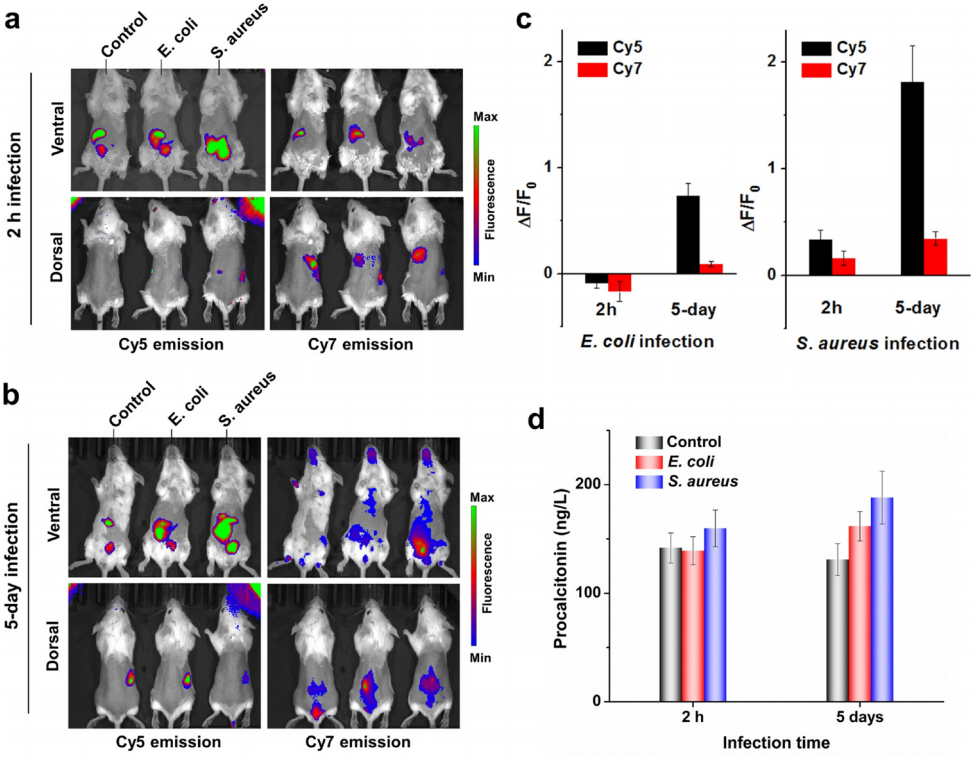

Figure 3. Multiple radical species profiling in living mice after bacterial infections. a, b) In vivo fluorescence signals of short-term (2 h) and long-term (5 days) mice infections post typical gram-negative and gram-positive bacteria injections, respectively. The probe molecule HCy5-Cy7 (0.05 mg mL^{-1} in saline, 200 μL) was injected via tail vein. Cy5 channel (λ_{Ex} = 640/680 nm); Cy7 channel ($\lambda_{Ex/Em}$ = 740/820 nm). c) The ratiometric fluorescence signal changes plot at Cy5 and Cy7 channels after the probe injection. Where $\Delta F = F_{bacteria} - F_0$, $F_{bacteria}$ indicates the total fluorescence intensity (ventral and dorsal) in the infected mouse, F_0 indicates the total fluorescence intensity (ventral and dorsal) in the control mouse. d) Serum procalcitonin tests (PCT) of short-term (2 h) and long-term (5 days) bacteria infected mice (n = 3).

time point, only *E. coli*-injected mice showed a slight decrease of the fluorescence at 800 nm, indicating the possibility of a low level of RNS production in the early-stage bacterial infection. To explore whether the nitrosative stress was appeared along with the bacterial pathogenesis, we injected HCy5-Cy7 after prolonged bacterial infection (e.g. 5 days). The results in Figure 3b and c clearly indicated the significant increase of the fluorescence signal at 660 nm, demonstrating the occurrence of oxidative stress at the long-term infection. However, only the minimum fluorescence change at 800 nm were observed. These results therefore evidence the ROS stress predominant pathogenesis in the process of the bacterial infection in the current model. In parallel, we also performed a clinical inflammation diagnostic test through the standard procalcitonin (PCT) method using mice blood samples to investigate the correlations between the status of bacterial infection and oxidative stress changes.[16] As expected, the serum procalcitonin level showed upward trends in the animals with prolonged infection of *E.coli* and *S. aureus* bacterial strains (Figure 3d), which was consistent with the results observed in the radical species-mediated fluorescence change in Figure 3c, clearly suggesting the good correspondence of pathological process with oxidative stress changes. There was no obvious procalcitonin enhancement observed in the short-term (e.g., 2 h) bacterial infections, probably originated from the relatively weak bacteria-pathological responses. Comparatively, HCy5-Cy7 demonstrated obvious fluorescent signal changes in the living mice along with bacterial infection, which could thus provide more sensitive and detailed outcomes for accurately profiling the pathology behind the bacterial infection progressions, especially for early detection of infectious diseases.

In conclusion, we have developed a unique NIR cyanine-dyad molecular probe HCy5-Cy7 that simultaneously reacted with radical species and triggered multispectral signal variations, which was further applied for multiplex manifestation of oxidative and nitrosative stress evolutions during the bacterial infections in live cells and living mice. The in vitro and in vivo results clearly disclosed the complex interplays of RONS during bacterial pathogenesis and the host-defense response. Overall, this study provides new perspectives for understanding the intrinsic correlations of oxidative/nitrosative stress and bacterial pathogenesis, which may contribute to current imaging-guided precision medicine in the fight against infectious diseases.

Acknowledgements

The authors sincerely thank Dr. John Chen from National University of Singapore and Dr. Yuan Qiao from Nanyang Technological University for the generous sharing of GFP-labeled bacterial strains for the phagocytosis study. B.X. acknowledges the financial supports from Tier 1 RG6/20, MOE 2017-T2-2-110, A*Star SERC A1983c0028, A20E5c0090, awarded in Nanyang Technological University (NTU), and National Natural Science Foundation of China (NSFC) (No. 51929201). M.B.C and W.Z. acknowledge the financial supports from ASTAR RIE2020 Advanced Manufacturing and Engineering (AME) IAP-PP Specialty Chemicals Programme Grant (No. A1786a0032) and MOE Tier 3 Grant (MOE2018-T3-1-003).

Conflict of interest

The authors declare no conflict of interest.

Keywords: bacterial infections · multiple radical dynamics · NIR fluorescence imaging · small-molecule probes

[1] a) S. B. Levy, B. Marshall, *Nat. Med.* **2004**, *10*, S122; b) R. Laxminarayan, P. Matsoso, S. Pant, C. Brower, J.-A. Røttingen, K. Klugman, S. Davies, *Lancet* **2016**, *387*, 168; c) J. Wang, D. L. Cooper, W. Zhan, D. Wu, H. He, S. Sun, S. T. Lovett, B. Xu, *Angew. Chem. Int. Ed.* **2019**, *58*, 10631; *Angew. Chem.* **2019**, *131*, 10741.

[2] a) A. Zychlinsky, P. Sansonetti, *J. Clin. Invest.* **1997**, *100*, 493; b) M. R. Parsek, P. K. Singh, *Annu. Rev. Microbiol.* **2003**, *57*, 677.

[3] a) F. C. Fang, *Nat. Rev. Microbiol.* **2004**, *2*, 820; b) B. Halliwell, *Trends Biochem. Sci.* **2006**, *31*, 509.

[4] a) H. Lindgren, S. Stenmark, W. Chen, A. Tärnvik, A. Sjöstedt, *Infect. Immun.* **2004**, *72*, 7172; b) S. Subbian, P. K. Mehta, S. L. Cirillo, L. E. Bermudez, J. D. Cirillo, *Infect. Immun.* **2007**, *75*, 127; c) O. Handa, Y. Naito, T. Yoshikawa, *Inflammation Res.* **2010**, *59*, 997.

[5] a) M. S. Riddle, H. L. DuPont, B. A. Connor, *Am. J. Gastroenterol.* **2016**, *111*, 602; b) R. L. Kradin, *Diagnostic Pathology of Infectious Disease E-Book*, 2nd ed., Elsevier Health Sciences, **2017**, p. 712.

[6] a) J. V. Frangioni, *Curr. Opin. Chem. Biol.* **2003**, *7*, 626; b) J. K. Willmann, N. Van Bruggen, L. M. Dinkelborg, S. S. Gambhir, *Nat. Rev. Drug Discovery* **2008**, *7*, 591; c) X. Wang, P. Li, Q. Ding, C. Wu, W. Zhang, B. Tang, *Angew. Chem. Int. Ed.* **2019**, *58*, 4674; *Angew. Chem.* **2019**, *131*, 4722; d) W. Sun, M. Li, L. Fan, X. Peng, *Acc. Chem. Res.* **2019**, *52*, 2818; e) S. He, J. Song, J. Qu, Z. Cheng, *Chem. Soc. Rev.* **2018**, *47*, 4258; f) L. Shi, Y. Wang, C. Zhang, C. Lu, B. Yin, Y. Yang, X. Gong, L. Teng, Y. Liu, X. Zhang, G. Song, *Angew. Chem. Int. Ed.* **2021**, *60*, 9562; *Angew. Chem.* **2021**, *133*, 9648; g) Z. Wang, Z. Xu, K. Upputuri, Y. Jiang, J. Lau, M. Pramanik, K. Pu, B. G. Xing, *ACS Nano* **2019**, *13*, 5816.

[7] a) T. A. Sasser, A. E. Van Avermaete, A. White, S. Chapman, J. R. Johnson, T. Van Avermaete, S. T. Gammon, W. M. Leevy, *Curr. Top. Med. Chem.* **2013**, *13*, 479; b) E. Moison, R. Xie, G. Zhang, M. D. Lebar, T. C. Meredith, D. Kahne, *ACS Chem. Biol.* **2017**, *12*, 928; c) B. Xing, A. Khanamiryan, J. Rao, *J. Am. Chem. Soc.* **2005**, *127*, 4158; d) W. M. Leevy, S. T. Gammon, H. Jiang, J. R. Johnson, D. J. Maxwell, E. N. Jackson, M. Marquez, D. Piwnica-Worms, B. D. Smith, *J. Am. Chem. Soc.* **2006**, *128*, 16476; e) X. Ning, S. Lee, Z. Wang, D. Kim, B. Stubblefield, E. Gilbert, N. Murthy, *Nat. Mater.* **2011**, *10*, 602; f) M. Van Oosten, T. Schäfer, J. A. Gazendam, K. Ohlsen, E. Tsompanidou, M. C. De Goffau, H. J. Harmsen, L. M. Crane, E. Lim, K. P. Francis, *Nat. Commun.* **2013**, *4*, 2584; g) F. J. Hernandez, L. Huang, M. E. Olson, K. M. Powers, L. I. Hernandez, D. K. Meyerholz, D. R. Thedens, M. A. Behlke, A. R. Horswill, J. O. McNamara II, *Nat. Med.* **2014**, *20*, 301; h) A. R. Akram, N. Avlonitis, A. Lilienkampf, A. M. Perez-Lopez, N. McDonald, S. V. Chankeshwara, E. Scholefield, C. Haslett, M. Bradley, K. Dhaliwal, *Chem. Sci.* **2015**, *6*, 6971.

[8] a) C. M. Sadlowski, S. Maity, K. Kundu, N. Murthy, *Mol. Syst. Des. Eng.* **2017**, *2*, 191; b) X. Chen, K.-A. Lee, X. Ren, J.-C. Ryu, G. Kim, J.-H. Ryu, W.-J. Lee, J. Yoon, *Nat. Protoc.* **2016**, *11*, 1219; c) R. Olekhnovitch, B. Ryffel, A. J. Müller, P. Bousso, *J. Clin.*

Invest. **2014**, *124*, 1711; d) Z. Song, D. Mao, S. H. Sung, R. T. Kwok, J. W. Lam, D. Kong, D. Ding, B. Z. Tang, *Adv. Mater.* **2016**, *28*, 7249.

[9] a) J. van der Heijden, E. S. Bosman, L. A. Reynolds, B. B. Finlay, *Proc. Natl. Acad. Sci. USA* **2015**, *112*, 560; b) S. Suri, S. M. Lehman, S. Selvam, K. Reddie, S. Maity, N. Murthy, A. J. García, *J. Biomed. Mater. Res. Part A* **2015**, *103*, 76.

[10] a) X. Ai, Z. Wang, H. Cheong, Y. Wang, R. Zhang, J. Lin, Y. Zheng, M. Gao, B. Xing, *Nat. Commun.* **2019**, *10*, 1087; b) K. Kundu, S. F. Knight, N. Willett, S. Lee, W. R. Taylor, N. Murthy, *Angew. Chem. Int. Ed.* **2009**, *48*, 299; *Angew. Chem.* **2009**, *121*, 305; c) J. Peng, A. Samanta, X. Zeng, S. Han, L. Wang, D. Su, D. T. Loong, N. Kang, S. J. Park, A. H. All, *Angew. Chem. Int. Ed.* **2017**, *56*, 4165; *Angew. Chem.* **2017**, *129*, 4229; d) Z. Wang, X. Ai, Z. Zhang, Y. Wang, X. Wu, R. Haindl, E. Y. Yeow, W. Drexler, M. Gao, B. Xing, *Chem. Sci.* **2020**, *11*, 803.

[11] a) D. Oushiki, H. Kojima, T. Terai, M. Arita, K. Hanaoka, Y. Urano, T. Nagano, *J. Am. Chem. Soc.* **2010**, *132*, 2795; b) P. Gao, W. Pan, N. Li, B. Tang, *Chem. Sci.* **2019**, *10*, 6035; c) X. Jiao, Y. Li, J. Niu, X. Xie, X. Wang, B. Tang, *Anal. Chem.* **2018**, *90*, 533; d) X. Bai, K. K.-H. Ng, J. J. Hu, S. Ye, D. Yang, *Annu. Rev. Biochem.* **2019**, *88*, 605; e) B. Li, L. Lu, M. Zhao, Z. Lei, F. Zhang, *Angew. Chem. Int. Ed.* **2018**, *57*, 7483; *Angew. Chem.* **2018**, *130*, 7605; f) D. Li, S. Wang, Z. Lei, C. Sun, A. M. El-Toni, M. S. Alhoshan, Y. Fan, F. Zhang, *Anal. Chem.* **2019**, *91*, 4771; g) W. Sun, S. Guo, C. Hu, J. Fan, X. Peng, *Chem. Rev.* **2016**, *116*, 7768.

[12] X. Jia, Q. Chen, Y. Yang, Y. Tang, R. Wang, Y. Xu, W. Zhu, X. Qian, *J. Am. Chem. Soc.* **2016**, *138*, 10778.

[13] a) N. M. Iovine, S. Pursnani, A. Voldman, G. Wasserman, M. J. Blaser, Y. Weinrauch, *Infect. Immun.* **2008**, *76*, 986; b) T. Salonen, O. Sareila, U. Jalonen, H. Kankaanranta, R. Tuominen, E. Moilanen, *Br. J. Pharmacol.* **2006**, *147*, 790.

[14] a) Q. Xu, C. H. Heo, G. Kim, H. W. Lee, H. M. Kim, J. Yoon, *Angew. Chem. Int. Ed.* **2015**, *54*, 4890; *Angew. Chem.* **2015**, *127*, 4972; b) A. Kaur, J. L. Kolanowski, E. J. New, *Angew. Chem. Int. Ed.* **2016**, *55*, 1602; *Angew. Chem.* **2016**, *128*, 1630; c) H. Maeda, K. Yamamoto, Y. Nomura, I. Kohno, L. Hafsi, N. Ueda, S. Yoshida, M. Fukuda, Y. Fukuyasu, Y. Yamauchi, *J. Am. Chem. Soc.* **2005**, *127*, 68; d) K. M. Robinson, M. S. Janes, M. Pehar, J. S. Monette, M. F. Ross, T. M. Hagen, M. P. Murphy, J. S. Beckman, *Proc. Natl. Acad. Sci. USA* **2006**, *103*, 15038; e) B. C. Dickinson, D. Srikun, C. J. Chang, *Curr. Opin. Chem. Biol.* **2010**, *14*, 50; f) X. Chen, F. Wang, J. Y. Hyun, T. Wei, J. Qiang, X. Ren, I. Shin, J. Yoon, *Chem. Soc. Rev.* **2016**, *45*, 2976.

[15] M. J. Sweet, D. A. Hume, *J. Leukocyte Biol.* **1996**, *60*, 8.

[16] L. Simon, F. Gauvin, D. K. Amre, P. Saint-Louis, J. Lacroix, *Clin. Infect. Dis.* **2004**, *39*, 206.

Manuscript received: March 23, 2021
Revised manuscript received: May 12, 2021
Accepted manuscript online: May 21, 2021
Version of record online: June 28, 2021

